RSC Advances

PAPER

View Article Online
View Journal | View Issue

Cite this: *RSC Adv.*, 2024, **14**, 872

Surface plasma modification of cellulose acetate fiber filter for the adsorption of typical components in smoke components†

Baoxin Shao,[a] Xing Wu,[a] Kangzhong Shi,[b] Ying Zhao,*[b] Jie Huang,[c] Wenjie Zhou,[c] Mengdie Cai[c] and Lisheng Guo*[c]

Received 8th November 2023
Accepted 15th December 2023

DOI: 10.1039/d3ra07624e

rsc.li/rsc-advances

Surface modification of cellulose acetate filter rods with low temperature plasma was performed to explore the retention and adsorption effect of modified filter rods on typical components (CO, H_2O, benzene, and formaldehyde) in cigarette smoke. The surface structure and composition of the cellulose acetate filter rods were modified by changing the plasma treatment time. The modified filter rods were characterized by N_2 physical adsorption (BET), scanning electron microscopy (SEM), X-ray diffraction (XRD), X-ray photoelectron spectroscopy (XPS), contact angle of H_2O, Fourier transform infrared spectroscopy (FTIR) and *in situ* DRIFTS. Various functional groups were found on the surface of filter rods with the introduction of plasma modification, which exhibited strong retention performance for water vapor in cigarette smoke at room temperature and significantly enhanced adsorption for harmful substances (CO, benzene, and formaldehyde) in cigarette smoke.

1. Introduction

Cigarette smoke is a kind of aerosol, which contains thousands of compounds such as nicotine, tar, particulate matter (PM), heavy metals (arsenic, chromium, cadmium, lead, *etc.*), polycyclic aromatic hydrocarbons, *etc.* There are many carcinogens and other harmful components, which exist in the particulate phase and gas phase. This toxic smoke from cigarette inhalation is a major cause of many cancers and diseases, such as asthma, high blood pressure and so on.[1,2] Therefore, to improve the safety and quality of cigarettes, various strategies have been adopted to meet consumer needs. Cellulose acetate filter rods can effectively capture harmful substances in cigarette smoke, and the rational design of efficient filter rods is of great significance for reducing the concentration of harmful components in cigarette smoke. Surface modification engineering has important applications in reducing hazards. The development of a new type of filter material with high adsorption and high retention is the key problem to reduce the harmful composition of smoke.[3] In recent years, additives have been widely used in filter rod surface modification because of their high specific surface area, surface chemical properties and controllable morphology. Using low temperature plasma to modify the surface of acetate fiber filter rods is also a promising strategy. When the surface of the material is treated by plasma, all physical and chemical changes occur on the surface of the material, which can maintain the original advantages of the material and overcome its disadvantages. Compared with traditional modification methods, low temperature plasma modification has the advantages of low energy consumption, low investment and simple operation, so it is widely used in various materials. However, the research on filter rod surface modification with plasma is seldom paid enough attention.[4]

Low-temperature plasma generally produces ionized particles and energy by ionizing certain gases. Air, nitrogen, oxygen, argon, helium, fluorine, chloride and other compound gases have been successively applied to material surface modification.[5–8] When the surface of the material is treated by low temperature plasma, high-energy particles and light radiation will be generated to bombard the surface of the material, resulting in etching on the surface of the material and at the same time, chemical bonds will break and generate free radicals. Energy particles and energy light radiation can easily cause a series of physicochemical reactions in materials such as desorption, doping, etching, sputtering and degradation, cross-linking, surface grafting and interfacial polymerization.[9–11] On the one hand, oxygen-containing functional groups such as C–O, C=O and O–H will be introduced into the surface of the material after plasma treatment to enhance the surface wettability of the material.[12] Meanwhile, the surface structure and composition of the material will be changed, and then the surface energy of the material will be changed, resulting in the

[a]*Gansu Tobacco Industry Company Limited, Lanzhou, 730050, China*
[b]*Eastman Shuangwei Fibers Company Limited, Hefei, 230601, China. E-mail: zhaoy@esfcl.com*
[c]*Chemistry and Chemical Engineering, Anhui University School, Hefei, 230601, China. E-mail: lsguo@ahu.edu.cn*

† Electronic supplementary information (ESI) available. See DOI: https://doi.org/10.1039/d3ra07624e

increasing of the surface adhesion.[13] On the other hand, when the temperature is lower than 400 °C, the active particles and light radiation will decompose the reaction gas to generate deposits on the surface of the material, and cause changes in the surface properties of the material, thus changing its properties.[14]

Chen *et al.*[15] treated the outer surface of wheat straw by water vapor plasma, and the results showed that the outer surface of wheat straw after water plasma treatment became rough. A large number of free radicals were generated and oxygen-containing groups were introduced, and the initial contact angle, equilibrium contact angle, and total free energy of the surface were significantly increased. Chen *et al.*[16] used hexamethyldisiloxane low-pressure dielectric barrier discharge plasma to perform hydrophobic treatment on the surface of poplar wood. The ionized hexamethyldisiloxane reacted with free radicals on the surface of wood to form Si–O–Si and Si–O–C bond network structure, and the plasma produced needle-like nanostructures on poplar veneer. These factors synergistically improve the hydrophobicity of the poplar surface, and the equilibrium contact angle of the poplar was found to increase significantly. Jimenez *et al.*[17] used Ar cold plasma to initiate graft polymerization of phosphonate (DEVP) precursors coated on flexible polyurethane foam (PUF), and then subjected these PUFs to ultrasonic treatment, while the other group was not subjected to ultrasonic treatment. The PUF coating without ultrasonic treatment forms –PO free radicals under the action of plasma, which plays an important role in flame suppression, where the –H and OH free radicals formed by the decomposition of the substrate are easily removed, so no flame is generated in the combustion test. The FR mechanism after ultrasonic treatment was different, only the grafted DEVP appeared on the surface of PUF. Flames appeared first during the combustion test, but soon the flames were extinguished and charred without any dripping. Both sets of plasma-treated PUF coatings prevent foam dripping in combustion tests and promote carbonization and self-extinguishing after flame removal.

In this work, low temperature plasma was used to modify the filter rod material, and the effect of the modified filter rod on the retention of typical harmful components in flue gas was explored. The modification process is simple, convenient and easy to control. At the same time, different characterization techniques were used to study the effect of low temperature plasma treatment time on the adsorption and retention performance of filter rods.

2. Materials and methods

2.1 Material

The chemicals used in the experiment were purchased from Sinopharm Chemical Reagent Co., LTD. Purification of deionized water using a microporous system. The cellulose acetate filter rod (FR) used in this study obtained from China Tobacco Chongqing Industrial Company. Cellulose acetate has an acetyl substitution of about 2.4 and is supplied by Eastman Chemical Company. Its molecular formula is $[C_6H_7O_2(OCH_3)_x(OH)_{3-x}]$, n = 200–400). It is widely used commercially as a cigarette filter tow (cigarette cellulose acetate tow) with a radius of 4 mm and a length of 20 mm.

2.2 Surface modification

Plasma enhanced chemical vapor deposition (PECVD) equipment manufactured by Anhui Bayik Equipment Technology Co., LTD was used to process the plasma discharge of the sample. The whole instrument is mainly composed of air source, discharge chamber, vacuum system and plasma discharge system. Through the gases atmosphere (H_2: 10 vol%, Ar: 90 vol%), the quartz tube with 80 mm diameter is used as the discharge cavity, and the induction coupling coil is evenly wrapped on the surface of the cavity. Plasma discharge was performed on FR by changing the treatment temperature (50, 100, 150, and 200 °C) for 4 h. The obtained samples were labeled FR-50, FR-100, FR-150, and FR-200, respectively.

2.3 Material characterization

The microstructure of the samples was studied by field emission scanning electron microscopy (FE-SEM) and energy spectrometer (JSM-IT 700 HR, Japan). The AUTOSORB-1 device from Quantachrome Instruments was used to test the specific surface area and total pore volume at liquid nitrogen temperatures (−196 °C). Prior to the test, each sample was degassed under vacuum conditions at 200 °C for 6 h. X-ray diffraction (XRD) spectra of the samples were collected using the Rigaku RINT 2400 X-ray diffractometer (Cu-Ka, 40 kV, 40 mA). Scans are recorded in the 2θ range of 5–90° with a step size of 0.05°/s. The hydrophilicity and hydrophobicity of the samples were determined by a simple wet chemical method. Thereinto, wetting rate instead of water contact angle (also stands for hydrophilic and hydrophobic properties) were measured on DSA100M (Krüss instrument) in an environmental chamber saturated with water vapor under ambient conditions.

To investigate the adsorption properties of typical components over FR samples, *in situ* DRIFTS (diffuse reflectance-Fourier transform infrared technique) measurements were performed on Bruker IFS 66 v/s FTIR spectrometer. As shown in Fig. S1,† the device consists of a detection system, a reaction system and a coupled reaction gas metering system. In a gas dosing system, a mass flow controller is used to control 20 vol% O_2/N_2 compressed air that carries SR vapor from a saturator containing typical components such as acetone. Water vapor is supplied through a bypass line and regulated to the battery. The cell system consists of a mantis DRIFTS attachment (Harrick Scientific) and a pool (HVC, Harrick Scientific). The tank is equipped with a sample cup with a fixed plate inside and is covered by a dome with three Windows. Cooling water circulates through coils around the bottom of the dome to facilitate the reaction at room temperature.

3. Results

To explore the influences of controlled treatment temperature on morphologies and structures under the condition of plasma modification, N_2 physical adsorption measurements were used

to study the structure of reference FR and surface functionalized FR-X (X = 50, 100, 150 and 200 °C) samples. Detailed results are summarized in Fig. 1 and Table 1. As seen, all FR samples present low surface area regardless of plasma modification. However, the difference of specific surface area increases with the increase of treatment temperature (50–150 °C), while the specific surface area decreases as the temperature further increases. Combined with the changes of pore volume, the pore volume of the sample first shrank and then expanded after 50–150 °C treatment. After 200 °C treatment, the formed were destroyed, resulting in a decrease in the specific surface area and pore volume of the material. Meanwhile, the pore sizes of all samples were in the range of 2.03–6.2 nm.

In order to further observe whether the morphologies of plasma-modified FR samples treaded by different temperature, scanning electron microscopy (SEM) was used (Fig. 2). For FR samples without any modification, it consists of many irregularly shaped polyhedra with a diameter of about 50 μm. Local magnification shows that FR has good surface smoothness. After plasma modification with different temperature, the changes of sample surface morphologies and structures can be ignored. The surface smooth characteristics are still maintained with no obvious pores, indicating that plasma treatment has little effect on the physical morphologies and structures of samples.

To compare the phase composition of the prepared FR samples, the samples were characterized by X-ray diffraction (XRD). According to XRD results, all FR samples exhibit the same amorphous peak structure between 5 and 50 degrees (Fig. 3). Obviously, compared with reference FR sample, the phase composition of FR sample was not changed after plasma modification. As discussed above, plasma modification usually modifies functional groups on the surface, thereby affecting material properties, which is consistent with XRD results. Combined with BET, XRD and SEM (Fig. 1–3), it can be inferred that the modified properties of the material are unlikely to come from the physical structure and composition characteristics to some extent.

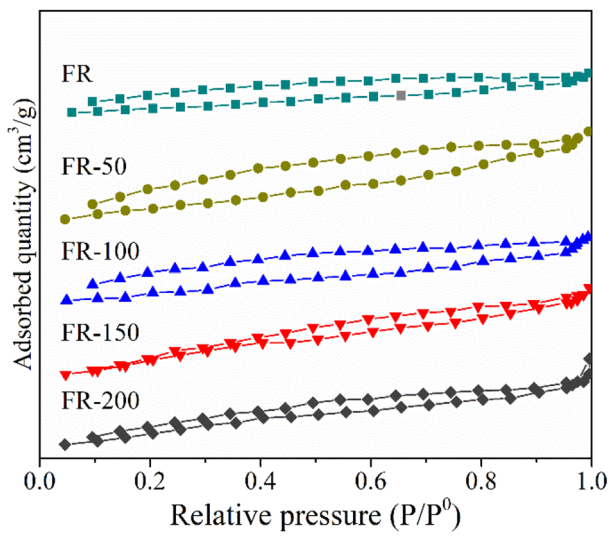

Fig. 1 N_2 adsorption–desorption isotherms of different FR samples.

Table 1 Structural characteristics of different FR samples

Samples	A_{BET} ($m^2\ g^{-1}$)	V_{total} ($cm^3\ g^{-1}$)	$D_{pore\text{-}size}$ (nm)
FR	1.27	0.0013	4.27
FR-50	2.01	0.0031	6.20
FR-100	2.04	0.0022	4.47
FR-150	6.01	0.0030	2.03
FR-200	3.06	0.0025	3.27

The hydrophilicity and hydrophobicity of the material can usually reflect the surface characteristics of the microenvironment of the material. For example, materials with a rich hydroxyl group (–OH) on their surface have a strong affinity for water molecules. In general, the moisture content in the smoke plays a crucial role in the smoke taste. In addition, some typical harmful organic compounds in the flue gas can be combined with the surface hydroxyl group, which can reflect the possible retention characteristics of harmful substances on the surface by improving the hydrophilic and hydrophobic characteristics of the material. Therefore, it is necessary to investigate the hydrophilicity of the plasma modified FR surface. The main component of FR is cellulose acetate, which is loose in texture and easy to absorb H_2O, and can not meet the routine test requirements of surface water drop contact angle. To overcome this issue, the hydrophilicity and hydrophobicity of the FR samples are inferred from the wetting rate. As shown in Fig. 4, the residence time of water droplets on the FR surface from the beginning to the end of water droplets penetration is less than 0.28 s. After plasma modification, the retention time of water

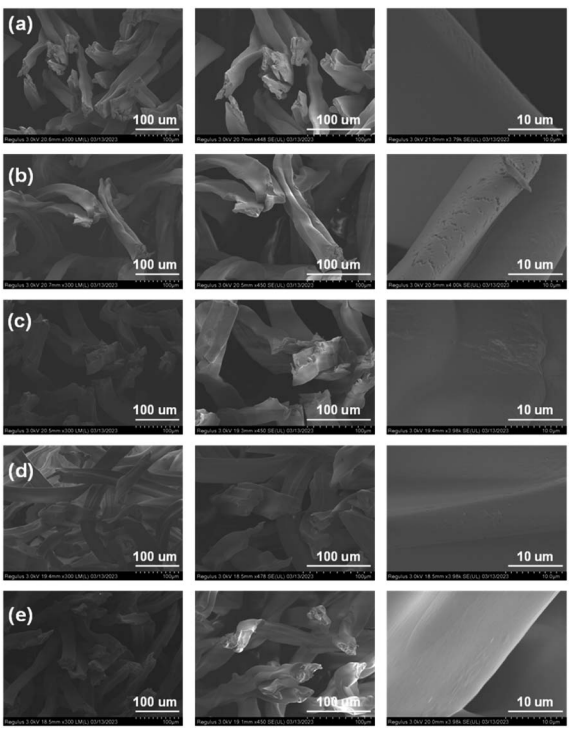

Fig. 2 SEM images of different FR samples. (a) FR, (b) FR-50, (c) FR-100, (d) FR-150, (e) FR-200.

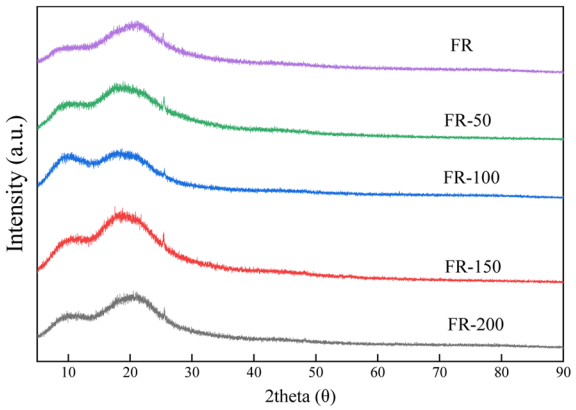

Fig. 3 XRD patterns of different FR samples.

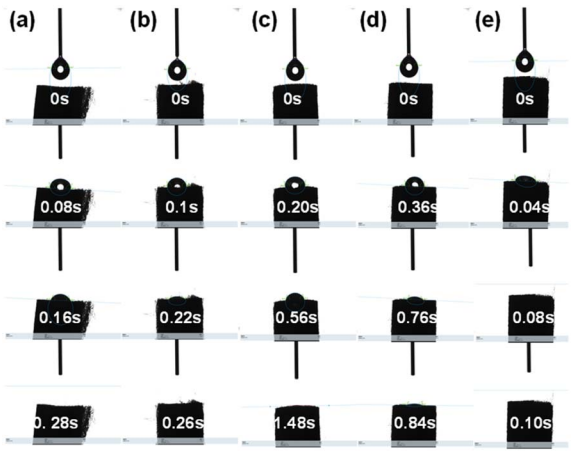

Fig. 4 Hydrophilicity and hydrophobicity of different FR samples based on dynamic wetting rate measurements. (a) FR, (b) FR-50, (c) FR-100, (d) FR-150, (e) FR-200.

droplets on FR surface increased significantly. With the further increase of plasma modification treatment temperature (50–200 °C), the residence time of water droplets first increased and then decreased, reaching the maximum value of 1.48 s in FR-100 sample. Interestingly, when the plasma treatment time reaches 200 °C, its water droplet retention time is smaller than that of the FR sample without modification. This phenomenon may be due to the excessive plasma treatment temperature, which destroys the pore channel or reduces surface hydroxyl group of the filter rod. The results are consistent with the results of N_2 physical adsorption measurement (Table 1 and Fig. 1). The result shows that the hydrophilicity of FR material can be improved effectively by adjusting the temperature of plasma treatment. It can be seen that FR with plasma modification has a strong ability to trap water vapor in flue gas at room temperature.

X-ray photoelectron spectroscopy (XPS) was used to analyze surface chemical state of FR samples after plasma modification. The C 1s spectra of different FR samples were shown in Fig. 5(a)–(e). The compositions and surface groups were summarized in and Tables S1 and S2.† The binding energy of 284.8 eV is attributed to the C–C bond,[18] while high binding energy positions are attributed to the C–O, C=O and CO_3^{2-} bonds, respectively. Clearly, the compositions of surface atoms change slightly after the plasma modification, especially FR-100 sample (Table S1†). To further investigate the influences of plasma treatment, surface groups composition were also compared (Table S2†). Among them, the proportion of C–O in FR-100 sample increases significantly, and more hydroxyl groups may be generated on the sample surface, which is conducive to the adsorption of harmful polar substances in the flue gas. In fact, for the FR-100 sample, the dynamic wetting rate also supports this hypothesis (Fig. 4). It is worth noting that the influence of plasma treatment temperature on surface groups is not regular, and it is a comprehensive phenomenon of various surface changes. Fourier transform infrared spectroscopy (FTIR) is a relatively simple method to detect the types and contents of functional groups in samples. Fig. 5(f) shows the FTIR spectra of FR and FR-100. In the spectrum of FR samples, the strong band at 3400 cm^{-1} are attributed to –OH stretching.[28] The peak intensity of FR-100 sample is obviously stronger than that of FR sample, which indicates that a large number of –OH groups are formed in the modified sample.

Diffused Fourier transform infrared spectroscopy (DRIFTS) is a suitable *in situ* surface analysis technique. By tracking and characterizing the adsorption state of molecules on the surface of materials, valuable surface reaction information can be obtained, thus the analysis of reaction mechanism has been paid more and more attention in various fields, especially in the study of catalytic processes.[19] As a consequence, the adsorption

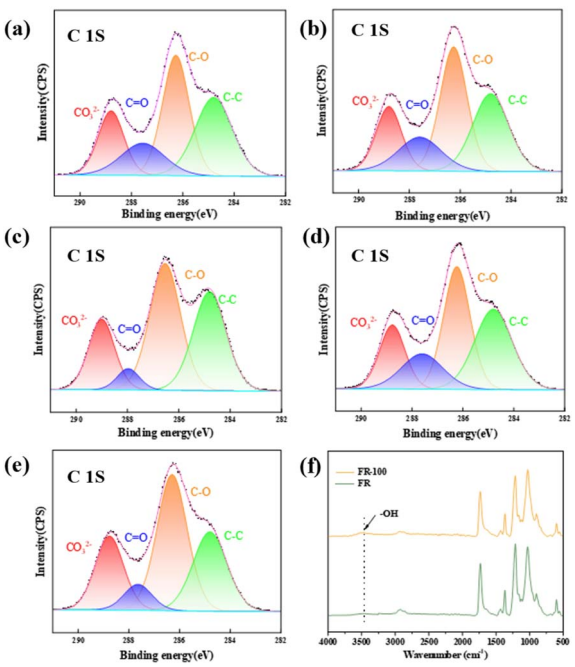

Fig. 5 X-ray photoelectron spectroscopy (XPS) of different FR samples. (a) FR, (b) FR-50, (c) FR-100, (d) FR-150, (e) FR-200, and (f) Fourier transform infrared spectroscopy (FTIR) of different FR samples.

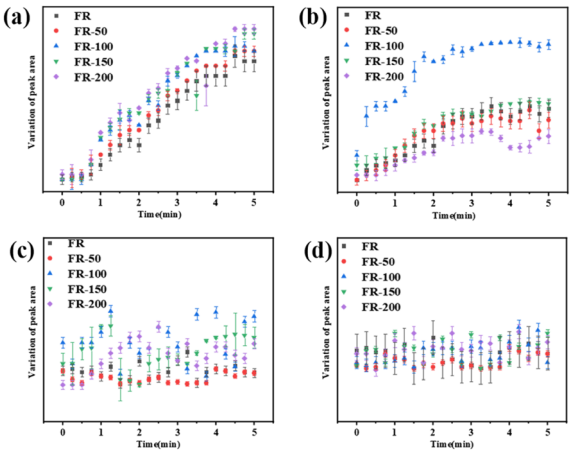

Fig. 6 Breakthrough curve adsorption on cellulose acetate rod with adsorption temperature based on *in situ* DRIFTS spectrum. (a) CO, (b) H_2O, (c) benzene, and (d) formaldehyde.

characteristics of typical flue gas components on different FR samples are studied by *in situ* DRIFTS technique (Fig. 6 and S2–S5†). First, CO, a typical harmful substance in flue gas, is used as the probe molecule to study the adsorption characteristics of different FR. As seen, the *in situ* DRIFTS spectra of CO on different FR surfaces at room temperature. The band at 2159 cm^{-1} belongs to the C=O stretching peak (Fig. S2†), which indicates that CO adsorbed on the FR surface after exposure to CO stream.[20–23] As shown in Fig. 6a, the C=O stretching peak of FR samples without any treatment is weak, and the C=O stretching peak of FR samples after plasma modification is significantly enhanced. *In situ* DRIFTS test shows that the CO adsorption of FR sample is enhanced after plasma modification. The IR band at 1035 cm^{-1} is assigned to the stretching vibration of ν as (–OH) (Fig. S3†).[24] The adsorption of –OH increased with the increase of plasma treatment temperature, and reached the maximum level at FR-100. Then the adsorption of –OH decreased and reached the lowest at FR-150, showing a volcanic-type distribution. It can be concluded that proper plasma treatment temperature can increase the adsorption and retention of H_2O, but too high plasma treatment temperature will destroy the structures of samples and weaken the adsorption of –OH. These findings are also consistent with the characterization of dynamic wetting rate measurements in Fig. 4. Gaseous benzene has an absorption band at 3038–3057 cm^{-1},[25] the adsorption of benzene on FR sample after plasma modification is not obvious, but the adsorption of benzene on FR-100 sample is slightly increased (Fig. 6c and S4†). The absorption bands at 1241 and 1010 cm^{-1} are considered as the characteristic absorption peaks of formaldehyde,[26,27] the adsorption of formaldehyde by all FR samples is not obvious(Fig. 6d and S5†).

4. Conclusions

The surface of cellulose acetate filter rod was modified by plasma modification technology aiming for the retention and adsorption of typical components in smoke. After modification, functional group of cellulose acetate filter rod were obviously changed. The specific surface area increases slightly with the increase of plasma treatment temperature (50–100 °C), but the specific surface area decreases after 150 °C of plasma treatment. After 50–150 °C treatment, the pore volume first shrank and then expands. After 200 °C treatment, the formed pores are destroyed, resulting in a decrease in the specific surface area and pore volume of the material. However, with the increase of plasma treatment temperature, the changes of the surface morphology and structure of the cellulose acetate filter rod can be ignored. It still maintains a good surface smooth characteristics and no obvious pores, but there is a small cavity formation after 50 °C and 100 °C treatment. Moreover, more –OH groups are formed on the surface of the FR-100 sample, which is conducive to the adsorption of harmful substances in the flue gas, which is also proved by *in situ* DRIFTS test. Cellulose acetate filter rod samples with plasma modification can enhance the adsorption of typical components in smoke, which sheds a light on the modified design of high efficiently filter rob for practical industry in future.

Conflicts of interest

The authors declare no conflict of interest.

Notes and references

1 S. K. Pandey, P. K. Vishwakarma, S. K. Yadav, P. Shukla and A. Srivastava, *ACS Appl. Nano Mater.*, 2019, **3**, 760–771.
2 M. Zhu, Q. Cao, B. Liu, H. Guo, X. Wang, Y. Han, G. Sun, Y. Li and J. J. C. Zhou, *Cellulose*, 2020, **27**, 3889–3902.
3 J. Cao, X. L. Ma, A. J. Yang and W. J. Xu, *Polym. Polym. Compos.*, 2006, **14**, 65–71.
4 J. Ganster and H. P. Fink, *Bio-Based Plastics: Materials and Applications*, 2013, pp. 35–62.
5 H. Kaczmarek, J. Kowalonek, A. Szalla and A. Sionkowska, *Surf. Sci.*, 2002, **507–510**, 883–888.
6 H.-C. Huang, D.-Q. Ye and B.-C. Huang, *Surf. Coat. Technol.*, 2007, **201**, 9533–9540.
7 D. S. Kim, J. E. Kim, W. O. Lee, J. W. Park, Y. J. Gill, B. H. Jeong and G. Y. Yeom, *Plasma Processes Polym.*, 2019, **16**, 1800118.
8 L. Y. Makhotkina and V. I. Khristoliubova, in *VIII All-Russian (With International Participation) Conference on Low Temperature Plasma in the Processes of Functional Coating Preparation*, IOP, 2017, vol. 789.
9 H. Puliyalil, G. Filipič and U. Cvelbar, *Plasma Processes Polym.*, 2016, **13**, 737–743.
10 J. K. Kim, S. H. Kang, S. I. Choi, S. H. Lee, K. N. Kim and G. Y. Yeom, *J. Nanosci. Nanotechnol.*, 2014, **14**, 9411–9417.
11 M. Chaudhari and J. C. Du, *J. Vac. Sci. Technol., A*, 2012, **30**, 061302.
12 A. Vesel, I. Junkar, U. Cvelbar, J. Kovac and M. Mozetic, *Surf. Interface Anal.*, 2008, **40**, 1444–1453.
13 K. Dimic-Misic, M. Kostic, B. Obradovic, A. Kramar, S. Jovanovic, D. Stepanenko, M. Mitrovic-Dankulov,

S. Lazovic, L. S. Johansson, T. Maloney and P. Gane, *Cellulose*, 2019, **26**, 3845–3857.
14 Y. H. Zhu, W. Wang, X. Y. Jia, T. Akasaka, S. Liao and F. Watari, *Appl. Surf. Sci.*, 2012, **262**, 156–158.
15 W. M. Chen, Y. C. Xu, S. K. Shi, Y. Z. Cao, M. Z. Chen and X. Y. Zhou, *Sci. Rep.*, 2018, **8**, 2279.
16 W. M. Chen, X. Y. Zhou, X. T. Zhang, J. Bian, S. K. Shi, T. Nguyen, M. Z. Chen and J. L. Wan, *Appl. Surf. Sci.*, 2017, **407**, 412–417.
17 M. Jimenez, N. Lesaffre, S. Bellayer, R. Dupretz, M. Vandenbossche, S. Duquesne and S. Bourbigot, *RSC Adv.*, 2015, **5**, 63853–63865.
18 A. W. Jatoi, I. S. Kim and Q. Q. Ni, *Carbohydr. Polym.*, 2019, **207**, 640–649.
19 L. S. Guo, X. H. Gao, W. Z. Gao, H. Wu, X. B. Wang, S. Sun, Y. X. Wei, Y. Kugue, X. Y. Guo, J. Sun and N. Tsubaki, *Chem. Sci.*, 2022, **14**, 171–178.
20 C. S. Deng, Q. Q. Huang, X. Y. Zhu, Q. Hu, W. L. Su, J. N. Qian, L. H. Dong, B. Li, M. G. Fan and C. Y. Liang, *Appl. Surf. Sci.*, 2016, **389**, 1033–1049.
21 G. Cheng, X. F. Tan, X. J. Song, X. Chen, W. X. Dai, R. S. Yuan and X. Z. Fu, *Appl. Catal., B*, 2019, **251**, 130–142.
22 X. J. Yao, Y. Xiong, W. X. Zou, L. Zhang, S. G. Wu, X. Dong, F. Gao, Y. Deng, C. J. Tang, Z. Chen, L. Dong and Y. Chen, *Appl. Catal., B*, 2014, **144**, 152–165.
23 T. K. Liu, Y. Y. Yao, L. Q. Wei, Z. F. Shi, L. Y. Han, H. X. Yuan, B. Li, L. H. Dong, F. Wang and C. Z. Sun, *J. Phys. Chem. C*, 2017, **121**, 12757–12770.
24 L. Y. Q. Luo, J. D. LaCoste, N. G. Khamidullina, E. Fox, D. D. Gang, R. Hernandez and H. Yan, *Surf. Sci.*, 2020, **691**, 121486.
25 X. Y. Wang, Y. Liu, T. H. Zhang, Y. J. Luo, Z. X. Lan, K. Zhang, J. C. Zuo, L. L. Jiang and R. H. Wang, *ACS Catal.*, 2017, **7**, 1626–1636.
26 S. Sun, J. J. Ding, J. Bao, C. Gao, Z. M. Qi and C. X. Li, *Catal. Lett.*, 2010, **137**, 239–246.
27 V. Lochar, *Appl. Catal., A*, 2006, **309**, 33–36.
28 P. Fei, L. Liao, B. Cheng and J. J. A. M. Song, *Anal. Methods*, 2017, **9**, 6194–6201.